

estimate for $x = x_{k-1}$. (For each k successive estimates of x_{k-1} were found to differ by less than 10^{-8} after 35 iterations of the algorithm.) Since there are again two possible values for each x_k , the manner of choosing them was similar to that of the previous example: for x_{-1} the root less than the x value producing a maximum for $f(x)$, i.e., less than 1, was selected, and for all $k \leq -1$, the root greater than 1 was chosen. In this case the point $x_{-12} \in I$ with $f^{12}(x_{-12}) = z$ and $f'(x_k) \neq 0$ for $-12 \leq k \leq -1$, was found for all $a > 16.999$ ($r > 2.833$ for (1.3b)).

Similarly treating the fixed points of f^2 as in Example 4.1 and applying Theorem 3.1 reveals that chaos should occur for $a > 15.250$ ($r > 2.724$). The value of r which May estimated is the dividing line between stability and chaos is $r = r^* \approx 2.692$. For (4.3), therefore, the value should be $a = \exp(r^*) \approx 14.765$. Again it is likely that finding snap-back repellers of f^{2^k} for larger integers k will yield chaos for a even closer to this estimated value.

EXAMPLE 4.3. We shall now attempt to apply Theorem 3.1 to several problems of the form (1.2) where $F: \mathbb{R}^2 \rightarrow \mathbb{R}^2$. To illustrate the technique involved, first consider the following two-dimensional generalization of the problem (4.1):

$$\begin{aligned}x_{k+1} &= (ax_k + by_k)(1 - ax_k - by_k) \\y_{k+1} &= x_k.\end{aligned}\tag{4.4}$$

This problem possesses no special biological significance, but was selected for investigation since it can be reduced to (4.1) when $b = 0$.

Since we are primarily interested in only the positive solutions of (4.4), we shall begin by restricting the parameters a and b in the following manner: let these parameters lie in the region R of the (a, b) -plane described by $R = \{(a, b): a, b \geq 0 \text{ and } a + b \leq 4\}$. Under these conditions the set $D = \{(x, y): 0 \leq x, y \leq \frac{1}{4}\}$ is invariant under F . In order to justify an application of Theorem 3.1, let us first examine the qualitative behavior of (4.4) for $(a, b) \in R$.

The local dynamics of difference schemes in a neighborhood of an equilibrium are dependent upon the Jacobian of the function involved. Computing the two fixed points of F , we find the trivial one: $x_k = y_k = 0$, and for $a + b > 1$ the positive fixed point: $x_k = y_k = (a + b - 1)/(a + b)^2$. Also, a simple calculation shows that:

$$DF(x, y) = \begin{bmatrix} a - 2a(ax + by) & b - 2b(ax + by) \\ 1 & 0 \end{bmatrix}$$

To compute the eigenvalues λ_1, λ_2 of F at a point (x, y) , therefore, we let $|DF(x, y) - \lambda I| = 0$ to obtain:

$$\lambda^2 - \lambda(a - 2a(ax + by)) - (b - 2b(ax + by)) = 0.\tag{4.5}$$

Evaluating (4.5) at $x = y = 0$, we see that for $a + b < 1$, $|\lambda_1|, |\lambda_2| < 1$ and thus $(0, 0)$ is stable in the region $R_1 = \{(a, b): a, b \geq 0, a + b < 1\}$. However, leaving the region R_1 across the line $a + b = 1$, one eigenvalue becomes greater than 1 making $(0, 0)$ unstable. Simultaneous with this is the appearance of the non-trivial fixed point $Z = (z, z)$ where $z = (a + b - 1)/(a + b)^2$, whose eigenvalues by (4.5) satisfy:

$$\lambda^2 + A\lambda + B = 0 \quad (4.6a)$$

where

$$A = \frac{a(a+b-2)}{a+b} \quad \text{and} \quad B = \frac{b(a+b-2)}{a+b}. \quad (4.6b)$$

Note that the simultaneous occurrence of an eigenvalue becoming greater than 1 with the appearance of a new fixed point is not arbitrary. In [5] this would be classified as a type (b) bifurcation of $(0, 0)$.

Solving (4.6a), it is not difficult to check that Z is stable for values of (a, b) close to the line $a + b = 1$. However, moving away from this line, there are two ways in which Z is likely to become unstable: (i) when both eigenvalues are real and one of them exceeds 1 in norm, while the other remains less, and (ii) when both eigenvalues, being complex conjugates, have norm greater than 1.

For case (i) we can find the curve in the (a, b) -plane along which both eigenvalues are real and one equals 1 in absolute value. Letting the solutions of (4.6a) equal ± 1 yields $B \pm A + 1 = 0$. Substituting the values of A and B given by (4.6b) implies either $a + b = 1$ or $b^2 - a^2 + 3a - b = 0$. The dynamics across $a + b = 1$ have already been discussed. The latter path, however, separates stability of Z from instability. The behavior across this curve will be discussed below.

For case (ii) note that if the solutions of (4.6a) are complex and equal 1 in norm then $B = 1$, and thus the path described by: $b^2 + (a - 3)b - a = 0$ also separates stability of Z from instability. Combining this with the result of case (i),

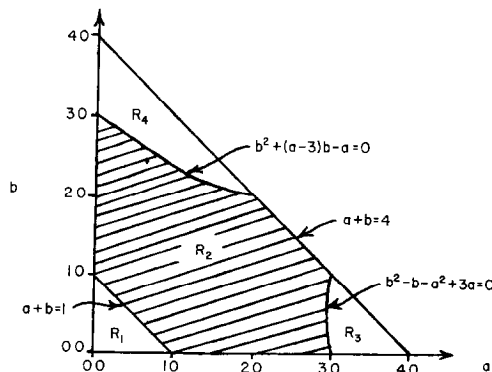


FIGURE 1

we see that Z is locally stable in the sub-region R_2 of R pictured in Fig. 1. In fact, numerical studies reveal that Z is globally stable in R_2 for $(x_0, y_0) \in D$.

We shall now investigate the dynamics of (4.4) for (a, b) in either R_3 or R_4 as pictured in Fig. 1. In the former-case crossing from R_2 into R_3 , one eigenvalue of $DF(Z)$ passes from greater to less than -1 . Numerical evidence suggests a type (a) bifurcation of Z , as described in [5], which doubles the period of an orbit, as a stable 2-cycle appears. Moving further to the right in R_3 , the stable 2-cycle itself becomes unstable and a bifurcation into a stable 4-cycle occurs. Passing in this way through R_3 , we observe successive bifurcation of 2^k -cycles into 2^{k+1} -cycles until we enter a sub-region of R_3 for which solutions of (4.4) are chaotic. Fig. 2 indicates the dynamics of (4.4) for $(a, b) \in R_3$. Note that for

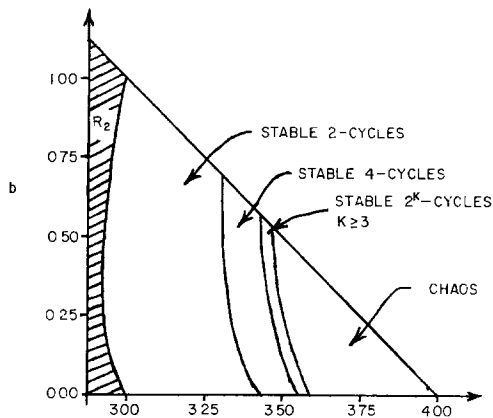


FIGURE 2

$b = 0$ the qualitative behavior of (4.4) conforms to that which May discovered for (1.3a).

Also note that it is not possible to explain the form of chaos which appears here by Theorem 3.1. This is evident by recalling that Z is unstable here only in the sense that one eigenvalue exceeds 1 in absolute value. Thus Z cannot be a snap-back repeller of F . The same is true of the fixed points of F^{2^k} for $k \geq 1$. Only one eigenvalue of DF^{2^k} at a point of the 2^k -cycle exceeds 1 in absolute value, and so again, Theorem 3.1 cannot be applied. We remark that the type of chaos that appears in R_3 can be explained by the same "twisted horseshoe" argument due to Guckenheimer, Oster and Ipaktchi [5].

Now let us examine (4.4) for $(a, b) \in R_4$. As previously described, the eigenvalues of $DF(Z)$ are complex and equal 1 in norm along the path separating R_2 from R_4 . Thus, according to [5], we might expect a type (c) bifurcation in which a stable continuous curve or an n -cycle for some n appears in the (x_k, y_k) -phase plane. As (a, b) crosses into R_4 , the eigenvalues of $DF(Z)$ cross the unit circle in the complex plane at certain angles with respect the positive real axis (one

angle being the negative of the other). If these angles are irrational multiples of π , then a stable continuous curve will appear around Z , and if they are rational multiples, a stable n -cycle for some n .

Numerical indications are that this does occur, and, in addition, as (a, b) moves further upward, the "radius" of these curves or cycles around Z increases. The visual shape of these trajectories also changes as we move deeper into R_4 in the manner described in [6]. At first the curves and cycles possess well formed circular shapes, but moving further into R_4 , although still remaining stable, they gradually develop several "kinked" areas. Figs. 3a and 3b illustrate the deformation a typical curve undergoes as (a, b) moves deeper into R_4 .

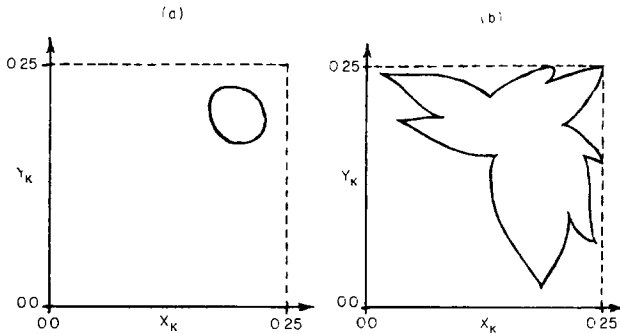


FIGURE 3

As might be expected, the stability of these curves and cycles vanishes and chaos appears, if (a, b) is moved far enough into R_4 . It is interesting to note that chaos here differs visually from that encountered in R_3 . In the latter case when (x_k, y_k) were plotted in phase plane, the result appeared to be one-dimensional chaos. That is, there exists a curve in the region D to which solutions of (4.4) tend as $k \rightarrow \infty$. However, on this curve there is chaotic behavior. Figure 4a depicts a typical pattern that is described for (a, b) in the chaotic

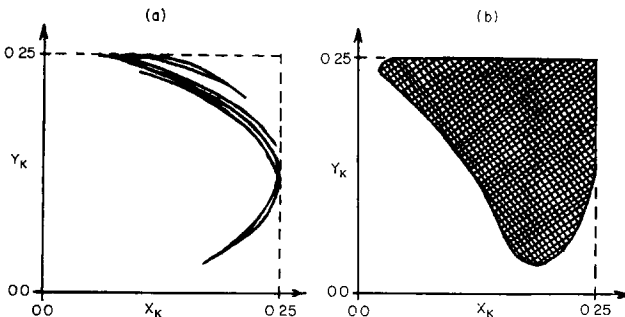


FIGURE 4

sub-region of R_3 . Notice its similarity to the "strange attractor" treated in [5]. On the other hand, for (a, b) in the chaotic sub-region of R_4 the iterates (x_k, y_k) tend to fill out an entire two-dimensional subset of D as $k \rightarrow \infty$. Figure 4b typifies this kind of chaos.

The qualitative behavior of (4.4) for $(a, b) \in R_4$ is shown in Fig. 5. As can be seen from this, in addition to the dynamics thus described, there is a sub-region

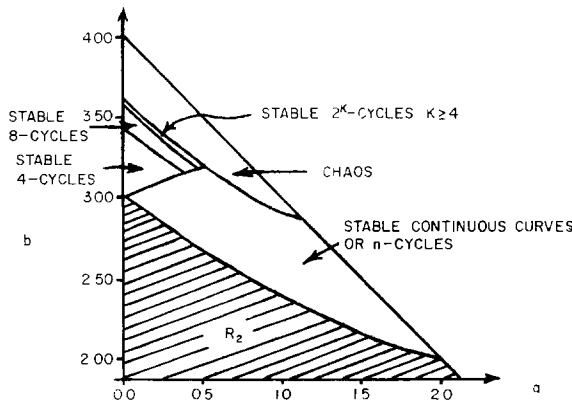


FIGURE 5

of R_4 in which the equation possesses stable 2^k -cycles for $k \geq 2$. Moving upward in this region, successive bifurcations (type (a)) of the 2^k -cycles into 2^{k+1} -cycles occur, until we again encounter chaos.

We shall now investigate this chaotic sub-region of R_4 . Since both eigenvalues of $DF(Z)$ exceed 1 in norm, there exists a neighborhood of Z in which this point is expanding and thus there is a possibility of using Theorem 3.1 to establish rigorously the chaotic behavior observed here. As was the case with Examples 4.1 and 4.2, we need to demonstrate the existence of a pre-image point (x_{-M}, y_{-M}) of Z , not equal to but lying in a neighborhood of Z in which the eigenvalues of DF exceed 1 in norm, and $|DF^M(x_{-M}, y_{-M})| \neq 0$. Also as before, we shall first provide an acceptable neighborhood $B_r(Z)$ for all (a, b) of interest.

Let $x = z + \epsilon$ and $y = z + \delta$. We shall show that the eigenvalues of $DF(x, y)$ are complex valued and exceed 1 in norm for all ϵ and δ sufficiently small. From (4.5) the eigenvalues of $DF(x, y)$ satisfy:

$$\lambda^2 + A_1\lambda + B_1 = 0 \quad (4.7)$$

where $A_1 = A + 2a(a\epsilon + b\delta)$ and $B_1 = B + 2b(a\epsilon + b\delta)$, and A and B are given by (4.6b). It can be estimated numerically that the imaginary parts of the eigenvalues of $DF(Z)$ exceed 1 in absolute value for $(a, b) \in R_4$.

Now, since $a + b \leq 4$, then:

$$\begin{aligned} A_1^2 - 4B_1 &< A^2 - 4B + 192(\epsilon + \delta) + 256(\epsilon + \delta)^2 \\ &< -1 + 192(\epsilon + \delta) + 256(\epsilon + \delta)^2. \end{aligned}$$

Therefore, choosing both $|\epsilon|$ and $|\delta|$ to be less than 10^{-3} is more than sufficient to insure that the roots of (4.7) are imaginary. Thus, their norms are given by: $\|\lambda_i\| = B_1 = B + 2b(a\epsilon + b\delta)$. Now, it is not difficult to check that throughout the region of observed chaos in R_4 , the norms of the eigenvalues of $DF(Z)$, which equal B , exceed 1.2 (e.g., one can solve $B = B(a, b) \geq 1.2$). Therefore, $\|\lambda_i\| > 1.2 - 32(\epsilon + \delta)$. Thus, choosing $|\epsilon|$ and $|\delta|$ to be less than 10^{-3} insures that the norms of the eigenvalues of $DF(x, y)$ exceed 1. So, we may take $B_r(Z)$ with $r = 10^{-3}$ to be our neighborhood.

In a manner similar to Example 4.1 the pre-images of Z can be found by letting $x_0 = y_0 = (a + b - 1)/(a + b)^2$ and inverting the function under consideration. In this case, the multi-valued inverse of (4.4) is given explicitly by:

$$\begin{aligned} x_{k-1} &= y_k, \\ y_{k-1} &= \frac{1 - 2ay_k \pm (1 - 4x_k)^{1/2}}{2b}. \end{aligned} \quad (4.8)$$

Again, as in previous examples, selecting the positive root for y_{-1} does not help to find an appropriate pre-image point of Z . Therefore, we shall again choose the negative root for y_{-1} , and the positive roots for all $k \leq -1$. As before, this selection appears to be optimal.

Numerically iterating (4.8) for a wide collection of points $(a, b) \in R_4$, with the selection of y_k 's made as described, reveals that the point (x_{-30}, y_{-30}) lies in $B_r(Z)$ with $r = 10^{-3}$ for those (a, b) values shown in Fig. 6. Also, the points

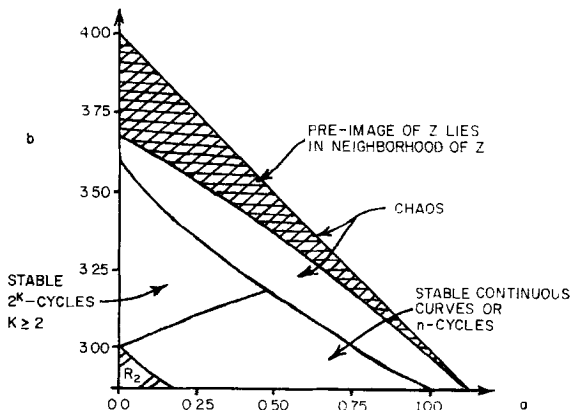


FIGURE 6

(x_k, y_k) satisfy $ax_k + by_k = \frac{1}{2}$ for $-30 \leq k \leq -1$. Since the line $ax + by = \frac{1}{2}$ describes the locus of points in D for which $|DF(x, y)| = 0$, we are thus guaranteed that $|DF(x_{-30}, y_{-30})| \neq 0$. Therefore, Z is a snap-back repeller here and Theorem 3.1 establishes chaos in this region of R_4 .

This same type of analysis can be performed upon the fixed points of the functions F^{2^k} for $k \geq 2$. In addition to the region of stable 2^k -cycles in Fig. 5 and 6, there exist unstable 2^k -cycles in that part of R_4 shown in Fig. 7 (above the

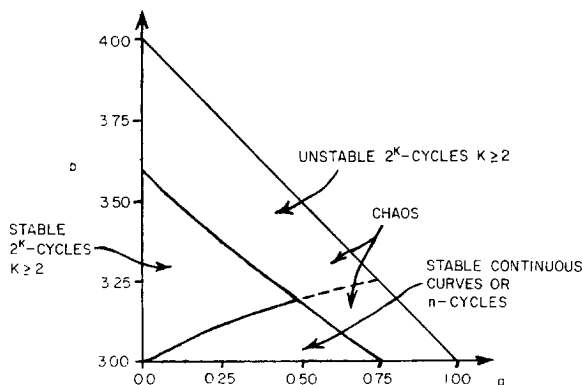


FIGURE 7

dotted line). In particular there are 4-cycles whose points are expanding under F^4 . Thus there is again a possibility of applying Theorem 3.1, this time to F^4 . Because of the complexity of the function involved, however, an ϵ, δ analysis of DF^4 close to a fixed point Z_4 of F^4 is virtually impossible. To investigate these points, therefore, the neighborhoods $B_r(Z_4)$ were numerically estimated for a large collection of (a, b) values covering the region of unstable 2^k -cycles. It was discovered that Z_4 is expanding under F^4 in $B_r(Z_4)$ with $r = 10^{-3}$ for all (a, b) of interest.

When graphed in the phase plane, the points of the 4-cycles are arranged roughly as the corners of a rectangle with sides parallel to the axes. Taking the element of the cycle closest to $(.25, 0)$ as the initial point (x_0, y_0) , the optimal sequence of roots of (4.8) appears to be the following: let y_{-1} have the positive root, and for all $k \leq -2$, let y_k have the root with sign equal to $\text{sgn}(-1)^m$, where m is the greatest integer less than or equal to $-(k+2)/2$. With this selection Fig. 8 illustrates the region in which the point (x_{-40}, y_{-40}) lies in $B_r(Z_4)$ where $Z_4 = (x_0, y_0)$ and $r = 10^{-3}$. It is likely that an investigation of the functions F^{2^k} for larger k values would establish chaos for the entire region in which the unstable 2^k -cycles reside. However, in these cases selecting the appropriate sequences of roots in (4.8), which involves a great deal of guesswork, seems very unlikely.

This same type of analysis could also be performed upon the points of the

n -cycles in the chaotic sub-region of R_4 shown in Figs. 7 and 8 (below the dotted line). But, again the problems introduced in the investigation of F^n for large values of n seem insurmountable.

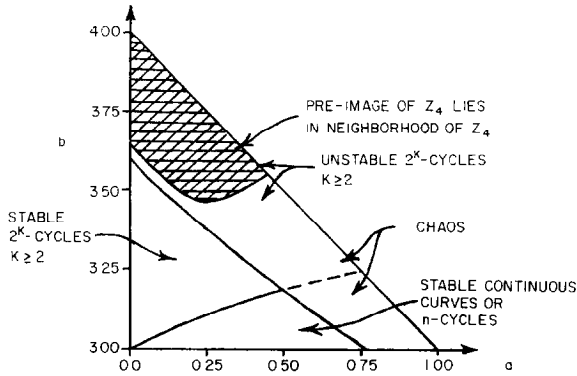


FIGURE 8

EXAMPLE 4.4. The two-dimensional difference scheme, (1.4), has been investigated in some depth by Guckenheimer, Oster and Ipaktchi. In particular they treat a special case of the equation by letting: $b_1 = b_2 = r$, $a = .1$ and $s = 1$. The resulting behavior is set out in [5]. Roughly, it is observed that, in a manner similar to the previous examples, as the parameter r is increased, the equation exhibits successive bifurcations from a stable equilibrium to a stable 3-cycle, from this 3-cycle to a stable 6-cycle, etc., until chaos is finally achieved. However, unlike previous cases, if r further increased, we observe the following pattern: regions of stability and successive bifurcations of $2^k n$ -cycles into $2^{k+1} n$ -cycles culminating in chaos, followed by a return of stability of $2^k n$ -cycles for larger values of n . The nature of the chaos observed here, however, is similar to that obtained in the region R_3 of Example 4.3, and thus cannot be investigated with respect to Theorem 3.1. A justification of chaos for these parameter values is provided in [5] by an argument similar to Smale's "horseshoe" example [7].

Therefore, consider the following modification of (1.4):

$$\begin{aligned} x_{k+1} &= (ax_k + by_k) \exp(-ax_k - by_k) \\ y_{k+1} &= x_k \end{aligned} \quad (4.9)$$

for which the parameter values will be restricted to the region $Q = \{(a, b): 0 \leq a \leq 1.5, 5 \leq b \leq 25\}$. Motivation for consideration of the region Q lies in the similarity of the form of (4.9) to that of (4.4), for which Theorem 3.1 established chaos for (a, b) close to the b -axis. So again we shall look in this region.